Compensating Printer Modulation Transfer Function in Spatial and Color Adaptive Rendering Workflows

Nicolas Bonnier *,** ***, Albrecht Lindner*** *,** ***, Christophe Leynadier*** * ***and Francis Schmitt*** **

*** Océ Print Logic Technologies S.A., Créteil, France.***

**** Institut TELECOM, TELECOM ParisTech, LTCI CNRS, France.***

nicolas.bonnier@oce.com, albrecht.lindner@oce.com, christophe.leynadier@oce.com, francis.schmitt@telecom-paristech.fr

Abstract

Experiments have shown that the quality of printed images depends on the capacity of the printing system to accurately reproduce details. We propose to improve the quality by compensating for the Modulation Transfer Function (MTF) of the printing system. The MTF of the printing system is measured using a modified version of the method proposed by Jang and Allebach [1]. Then the MTF is adaptively compensated in the Fourier domain, depending on the frequency and on the local mean value. This compensation is included within our mathematical framework for Spatial and Color Adaptive Gamut Mapping Algorithms. Results of a category judgment experiment show significant improvement as the printed MTF compensated images obtain the best scores.

Introduction

In the quest for an optimal reproduction of a color image, an impressive number of Gamut Mapping Algorithms (GMAs) have been proposed in the literature [2]. As preservation of the spatial details in an image is a very important issue for perceptual quality [3, 4], GMAs adaptive to the spatial content of the image, i.e. Spatial Gamut Mapping Algorithms (SGMAs), have been introduced [5]. These algorithms try to balance both color accuracy and preservation of details, by acting locally to generate a reproduction perceived as close to the original.

In order to perceptually assess the quality of the output of spatial gamut mapping algorithms, it is necessary to choose input and output gamuts and to process a selected set of images. The processed images are then reproduced on an output device, a monitor or a printing system (composed of a printer and a medium). The gamut of this device can correspond to the output gamut chosen to process the images. Such evaluations, using a printing system, have been conducted in [6–8]. Alternatively, a monitor simulating the gamut of a printing system can be used as in [9, 10]. The choice of a monitor over prints is often made for practical reasons as numerous images are compared in evaluation experiments and are more easily handled with a graphical user interface on a monitor. Liu et al. [11] advocate that soft-copy displays can adequately simulate hardcopy prints. Yet to evaluate the results we consider the ability of the algorithm to accurately reproduce both colors and spatial details. Therefore the output device should be able to reproduce adequately all the colors and the details in the processed images.

During preliminary experiments, we have compared the processed images reproduced on an Eizo Color Edge 221 monitor and with an Océ TCS 500 inkjet printer on standard Océ uncoated paper. We observed that images processed with SGMAs present significantly better details than images processed with pointwise GMAs when displayed on the monitor. Unfortunately, improvements are not as much significant when comparing prints on standard uncoated paper. It appears that the ability of the two systems (the monitor versus the printing system) to reproduce details are different, leading to strong differences in the perception of the spatial content in the resulting images. The ability of a system to reproduce details is captured in its Modulation Transfer Function (MTF), also called Spatial Frequency Response (SFR). The characterization and compensation of the MTF of printing systems are very important parts of high quality rendering workflows.

In this paper we first discuss the specificities of the printer MTF characterization, introduce the method chosen to characterize our device and present the resulting measurements. In the second section we present the compensation algorithm that we propose and how we include it in the spatial and color adaptive workflow. Finally the results of our category judgment experiment on the processed images are presented and commented.

Modulation Transfer Function

The MTF of a given system shows how much the system attenuates an input modulation signal. When considering a 1 dimensional (1D) spatial modulation, The MTF is defined as the ratio of the output amplitude $A_{out}(f)$ to the input amplitude $A_{in}(f)$:

$$MTF(f) \quad = \quad \frac{A_{out}(f)}{A_{in}(f)}, \tag{1}$$

where f is the spatial frequency component of the 1D signal. In order to describe a printing system, this ratio has to be measured for different frequencies and different orientations. For a given orientation of a modulation signal the results can be plotted in a graph where the ratio is plotted versus the frequency. For printing systems the ratio usually decreases as the frequency increases, showing the low-pass behavior of such devices wich tend to blur the details in images. An ideal imaging device would have an MTF constant at 1 for every frequency and orientation. In our preliminary experiments the MTF of the printing system was much lower than the MTF of the monitor. The technologies are indeed very different and the lower MTF of the printing system is mainly due to the halftoning algorithm and to the spreading of the ink on the paper.

Impact of the MTF of output devices

In a first large-scale evaluation experiment on a monitor [12], we noticed that it was difficult for the observers to compare original full input gamut images with smaller output gamut reproduc-

tions: color appearance of the simulated prints was not satisfying. Resulting data was noisy and seemed not trustable. Moreover the halftoning was not simulated on the monitor. It appeared then necessary to test SGMAs directly on printouts. However a low MTF can average out the gain of using a SGMA as suggested by results in [13].

In a second large-scale experimentation [14], in order to avoid the low MTF of the printing system we have simulated the gamut of the standard uncoated paper on a high-quality photo paper. The goal of this second experiment was to compare the SGMAs in a scenario where the gamut is limited but the MTF of the printing system is not an issue. Two *Spatial and Color Adaptive Gamut Mapping Algorithms* (SCAGMAs), introduced in [5, 14, 15] where evaluated in these psychophysical experiments. Results validate them in front of the SGMA proposed by Zolliker and Simon and two pointwise GMAs. Obviously the next step is to find ways to maintain the gain of using SCAGMAs in all situations, including in cases where the MTF is low.

Based on the above observations, we have started investigating on the MTF of the printing system aiming to improve the final printed results. An evaluation of existing characterization techniques and the results of the characterization of a printer has been published in [16]. Then we have included an additional step in the color and spatial adaptive rendering worflow to compensate for the diminution of details caused by the low modulation transfer function of the printing process.

Characterizing the Printer MTF

The MTF characterization of a printing system is not trivial: unlike digital capture devices, inkjet and laser printers are highly non-linear and therefore not easy to model. The MTF depends on different parameters related to the printing system (halftoning, addressability, dot size, quality of the medium) and on the characteristics of the input images. This is also related to the Nyquest-Shannon sampling theorem [17]. Usually a printing system has *low-pass* characteristics: mostly only high frequencies are attenuated and low frequencies are preserved.

Characterization of the MTF has been popular in photography and there are a few methods to measure the MTF for both silver-halide and digital image capture devices, in which sinusoidal and slanted-edge targets are used. These characterization methods have been standardized in [18] and [19]. While much effort has been spent in the characterization of the color characteristic curves of printing systems, until recently very little research [1, 20–22] has been published regarding the characterization of the MTF of printing systems. After a preliminary study [16, 23], we have selected the characterization method proposed by Jang and Allebach as it appears to be the most robust.

Jang and Allebach's Characterization

The method proposed in [1] consists of printing patches with sinusoidal patterns (see Figure 1), scanning them with a high resolution scanner and comparing their amplitudes with the values of constant tone patches. The value of these constant tone patches correspond to the maximum (max), the mean (bias) and the minimum (min) of the sinusoidal patches in the same row.

One row of the test image consists of these three constant tone patches followed by nine sinusoidal patches oscillating between the min and max value with frequencies set to $\{10, 20, 30, 40, 50, 60, 80, 100, 150\}$ cycles per inch, respectively. To measure the MTF with different biases, the test image consists of 19 rows. One row of the test image is illustrated in Figure 1. In the original test chart [1], the 19 bias values $b \in \mathscr{B} = \{b_1, b_2, \ldots, b_{19}\}$ are equidistantly distributes on L^*, the lightness scale of CIELAB which is an approximate psychometric color space. We have proposed in [16] to slightly modify the test chart to improve the reliability of the results: the bias values are equidistantly distributed in CIE XYZ, a colorimetric space better suited as it is more related to the physics of the measurement on the printing system. Furthermore, to lessen the influence of noise in the measurement, the amplitude of modulation of the sine waves is increased to $\Delta Y = 20$ (except for the extreme bias values to avoid clipping of the signal to either the paper white or the maximum black of the ink).

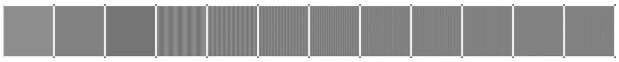

Figure 1. *Example of one single row of Jang and Allebach's test images.*

The characterization of a printing system can shortly be described as follows. We first scan the printout, then each row with constant mean gray level (bias) is processed separately.

1. Within one row the three constant tone patches are processed first. For each patch, its mean is calculated in the CIEXYZ space and converted into CIELAB values.
2. For each of the nine sinusoidal patches from the same row, the modulation signal is extracted by averaging the measured tristimulus values perpendicularly to the direction of modulation. The averaged values are converted to CIELAB values and projected on the line which connects the lower and upper mean values corresponding to the constant min and max tone patches, respectively.
3. Then, for all the points projected on the line the ΔE^*_{ab} distance to the lower mean value of the constant min patch is calculated. The result is a vector of ΔE^*_{ab} scalar values which is Fourier transformed. The amplitude of the main frequency of the patch is then extracted.
4. The amplitude is compared with the ΔE^*_{ab} distance between the constant min and max tone patches and it usually smaller. Since the scanner is not compensated at this point, their ratio is not yet the printer MTF. It is the MTF of the system composed by both the printer and the scanner.
5. For the scanner compensation we use the scanner MTF which has been separately measured with specific engraved patterns on a physical chart [19]. We then estimate how much the scanner attenuates a signal which oscillates between the min and max constant tone patches. This scanner ratio should be between 1 and the ratio calculated in the previous step. Dividing the first calculated combined printer and scanner ratio by the above scanner ratio provides the estimated compensated printer MTF.

Experimental MTF Measure

In our study we have used the inkjet printer Océ Colorwave 600 with standard Océ uncoated paper and an Epson scanner Expression 10000XL. Figure 2 shows the MTF characterization obtained with the modified Jang and Allebach test chart, aligned in

the horizontal directions. The MTF decreases as the frequency of the sine wave increases, as expected, but the MTF depends also on its bias or mean value: the MTF values are higher for medium gray levels than for high gray levels (high row indices) and slightly higher for low gray levels (low row indices). For this printer, the MTF values for the horizontal and vertical directions are similar.

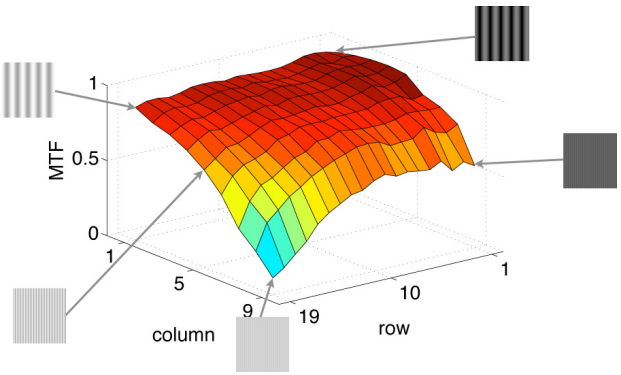

Figure 2. *Measured horizontal MTF of the Océ Colorwave 600, obtained with the modified Jang and Allebach test image (19 rows of increasing grey values (bias) x 9 columns of sine patterns increasing in frequency).*

Compensation in the Spatial and Color Adaptive Rendering Workflow

In the following sections we show how to embed the compensation of the MTF within the spatial and color adaptive rendering framework. We propose a compensation algorithm based on image decomposition which locally adjusts in an image the MTF compensation given the local mean for each pixel of that image.

SCACOMP

We consider now the Spatial and Color Adaptive COMPression algorithm (SCACOMP) [5, 15]. This algorithm is more robust to artifacts and faster to compute than SCACLIP, the other proposed SCAGMA. SCACOMP can be described by the diagram in Figure 3 and by the following process:

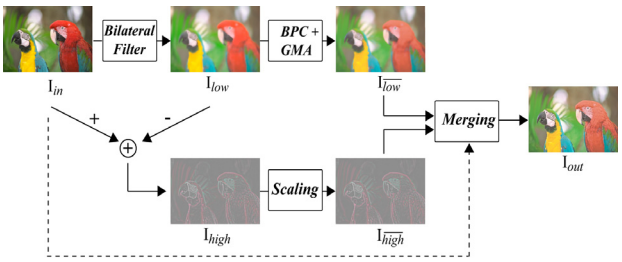

Figure 3. *Framework for new Spatial and Color Adaptive Gamut Mapping.*

1. Conversion of the original image to the CIELAB color space using the relative colorimetric intent of the input ICC profile: $\mathbf{I}_{in}$.
2. Decomposition in two bands using bilateral filtering (BF) [24]: $\mathbf{I}_{low}$ and $\mathbf{I}_{high}$.
3. Black Point Compensation (BPC) [25] and clipping of $\mathbf{I}_{low}$: $\mathbf{I}_{\overline{low}}$.
4. Adaptive scaling of $\mathbf{I}_{high}$: $\mathbf{I}_{\overline{high}}$.
5. Adaptive merging and mapping by color compression of $\mathbf{I}_{\overline{low}}$ and $\mathbf{I}_{\overline{high}}$: $\mathbf{I}_{out}$.
6. Conversion to the CMYK encoding of the output printer using the relative colorimetric intent of its ICC profile.

SCACOMP proposes an adaptive compression algorithm to preserve the color variations between neighboring pixels contained by $\mathbf{I}_{high}$. The concept is to project each color of pixel lying outside or near the boundary of the destination gamut $Gamut_{Dest}$ toward the 50% greypoint of $Gamut_{Dest}$ [26], more or less deeply inside the gamut depending on its neighbors.

In the Workflow

Under the assumption of a linear system, the degradation can be described by a multiplication in the Fourier domain. Assuming an input image I_{in}, its Fourier transform being $F(I_{in})$ and the system MTF, the fourier transform of the degraded image at the output is $F(I_{out}) = MTF\ F(I_{in})$. In the case where MTF is known at each frequency, the compensation is a simple division in the Fourier domain and the compensated input image $F(I_{comp})$ is then obtained by the inverse Fourier transform F^{-1} as follows:

$$I_{comp} \quad = \quad F^{-1}\left(\frac{F(I_{in})}{MTF}\right). \tag{2}$$

For simplicity and calculation speed we have embedded this division in the Fourier domain within the existing SCAGMA framework.

MTF Data In order to use the MTF data gathered in the previous section, it might be necessary to extrapolate missing extreme values [23]. In our experiment, the printing resolution is 600 dpi but the images are printed at 150 dpi, below the highest measured MTF value. Furthermore, the lowest measured frequency is 10 cycles per inch, and in our experiment, we set to 1 the MTF values between 0 and 10 cpi.

Color Space The MTF values have been measured for sine-wave modulations in the CIE XYZ space [23]. Yet the SCAGMA workflow is using the CIELAB color space and the division is applied in CIELAB. Since the Human Visual System (HVS) is more sensitive to luminance high frequency content than chrominance high frequency content, we propose to limit the deconvolution to the L^* channel.

Image decomposition One key aspect of the proposed SCAGMAs is the decomposition of the image in two bands, obtained by 5D Bilateral Filtering (BF) in the CIELAB space (see Figure 3). While the deconvolution can be applied before the image decomposition, we propose to apply it to the L^*_{high} channel of the high pass band to avoid producing halos or increasing the noise: L^*_{high} does not contain the sharpest edges of the input image $\mathbf{I}_{in}$. Deconvolution is inserted within the workflow, as shown in Figure 4: after the decomposition of the image $\mathbf{I}_{in}$ with the bilateral filter L^*_{high}, the L^* channel of the high frequency band $\mathbf{I}_{high}$, is selected. This channel is then transformed into Fourier space, divided through the printer MTF and transformed back. Then the image is recomposed by the adaptive merging and mapping.

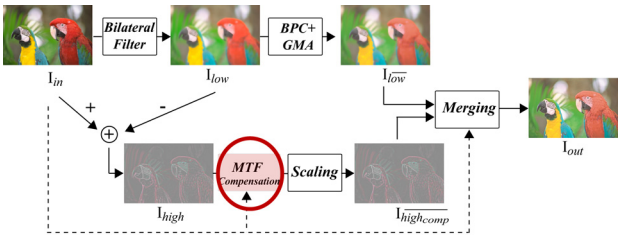

Figure 4. *MTF compensation within the Framework for Spatial and Color Adaptive Gamut Mapping.*

Locally Adaptive Compensation

The MTF values vary as a function of the bias, that is the mean gray level of the modulation signal. We propose to take into account the image local mean gray level as an estimation of the bias when compensating for the printer MTF: each pixel in L^*_{high} is compensated according to the local mean in $\mathbf{I}_{in}$.

$$L^*_{high_{comp}} = MTF_{comp}(L^*_{high}, L^*_{in}, MTF), \quad (3)$$

where $L^*_{high_{comp}}$ is the compensated L^* channel and MTF_{comp} the locally adaptive compensation.

Local mean A local measure of the mean gray level L^*_{in} is needed to achieve the locally adaptive compensation. Here we can take full advantage of the image decomposition and use $\mathbf{I}_{low}$ as an estimation of the local mean. Notice that values in $\mathbf{I}_{low}$ are obtained by bilateral filtering. This is an advantage as a local mean computed in $\mathbf{I}_{in}$ for a local detail in $\mathbf{I}_{high}$ should only be computed by using local and similar gray pixels, as this is done in $\mathbf{I}_{low}$ by the bilateral filter. Since the MTF was measured using modulation and bias values based on the CIE XYZ color space, $\mathbf{I}_{low}$ is converted to CIE XYZ and Y_{low} is taken as the local mean.

N deconvolutions of L^*_{high} The MTF has been measured for the bias values b_n, $n \in [1,N]$. Let MTF_n denotes the MTF measured for bias b_n. L^*_{high} can be divided through each $\mathrm{MTF}_n(f)$ in the Fourier domain which results in N compensated high pass images:

$$L^*_{\overline{high_n}} = F^{-1}\left(\frac{F(L^*_{high})}{K_{MTF_n}}\right),\ n \in [1,N], \quad (4)$$

where $L^*_{\overline{high_n}}$ is the compensated image in the image domain for bias value b_n.

Adaptive merging Then a locally adaptive merging can be processed for each pixel according to the local mean. The N compensated high pass bands $L^*_{\overline{high_1}}, \ldots, L^*_{\overline{high_N}}$ are merged to one single compensated high pass band $L^*_{high_{comp}}$.

Since only certain of the MTF values have been measured for a limited set of bias and frequency values, missing MTF values are fisrt linearly interpolated for the frequency range of the image sent to the printer ([0, 150] dpi in our experiments). Then for each pixel in $\mathbf{I}_{high}$ the two bias levels b_n and b_{n+1} closest to the value Y_{low} corresponding to that pixel are selected: $b_n \geq Y_{low} \geq b_{n+1}$ $L^*_{high_{comp}}$ is a linear interpolation between the compensated images $L^*_{\overline{high_n}}$ at these two bias levels:

$$L^*_{high_{comp}} = w \cdot L^*_{\overline{high_n}} + (1-w) \cdot L^*_{\overline{high_{n+1}}}, \quad (5)$$

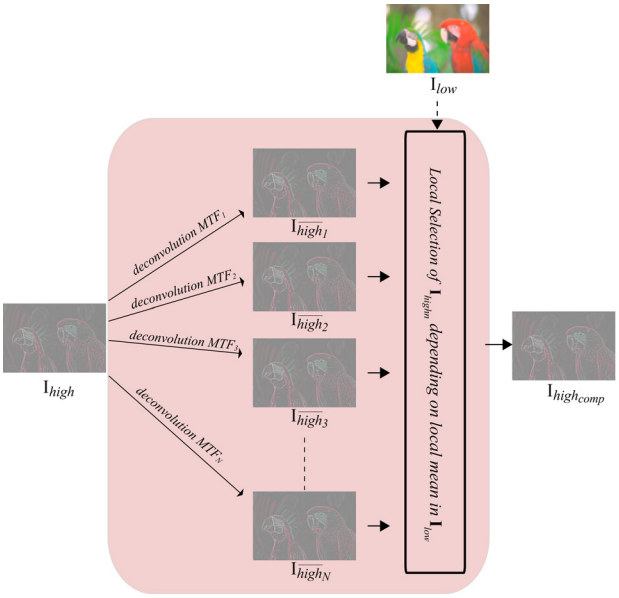

Figure 5. *Principle of the locally adaptive MTF compensation: the high-pass band $\mathbf{I}_{high}$ is compensated N times for MTF_n. Then for each pixel, a locally adaptive merging is processed according to the local mean estimated from $\mathbf{I}_{low}$.*

with:

$$w = \frac{Y_{low} - b_{n+1}}{b_n - b_{n+1}}. \quad (6)$$

Resuming SCAGMA process After the locally adaptive MTF compensation of L^*_{high}, the image $\mathbf{I}_{high_{comp}}$ is recomposed and scaled as follows [5]:

$$\mathbf{I}_{\overline{high_{comp}}} = Scaling(L^*_{high_{comp}}, C^*_{high}, h_{high}). \quad (7)$$

where C^*_{high} and h_{high} are the chroma and hue channels of $\mathbf{I}_{high}$. Then the SCAGMA process is resumed: MTF compensation is followed by an adaptive merging and mapping.

Psychophysical Experiment

The goal of this experiment was to evaluate the gain of the MTF compensation in spatial and color adaptive gamut mapping algorithms. After a preceding experiment [14], we have considered the inclusion of a black point compensation (BPC) in our framework [15]. To compare SCACOMP including BPC with other GMAs, we have applied BPC prior to each of the alternative GMAs in this experiment. Furthermore, to better evaluate the compensation and over compensation of the printer MTF, three alternative SCACOMP with various degrees of compensation have been included in this study. Therefore, the following 1 pointwise GMA and 4 SGMAs have been evaluated:

1. Black Point Compensation in CIE XYZ followed by HPMINΔE (hue-angle preserving minimum ΔE^*_{ab}) clipping in CIELAB. This combination is a baseline re-rendering algorithm in industry workflows. HPMINΔE was performed with the software ICC3D [27],

2. Z-HPMINΔE, proposed by Zolliker and Simon in [10], implemented using Black Point Compensation in CIE XYZ followed by HPMINΔE as the initial pointwise GMA and HPMINΔE as the second pointwise GMA,
3. SCACOMP with BPC in CIE XYZ,
4. SCACOMP-MTF with MTF Compensation,
5. SCACOMP-OVER with an over-compensation obtained by reducing the measured MTF by 20%, thus boosting the compensation by a factor $1/0.8 = 1.25$, or 25%.

Experiment Type and Observer Task In this category judgement experiment, the observers were presented 5 samples of a series of gamut mapped images along with a reference reproduction, they have to evaluate how close each reproduction is to the reference reproduction, on a scale of numbers from 1 to 7 where 1 represents the closest reproduction you can imagine and 7 represents the least accurate reproduction possible. A description of the accuracy for each level was proposed to help: 1) Most accurate you can imagine, 2) Highly accurate, 3) Very accurate, 4) Fairly accurate, 5) Moderately accurate, 6) Poorly accurate, 7) Least accurate reproduction possible. It was suggested to make your decision based on different parts of the image, to evaluate the fidelity of the reproduction of both colors and details, and look for possible artifacts. It is the accuracy of reproduction of the images which is evaluated, not the pleasantness.

Images A total of 15 images were used in this experiment: 7 sRGB images from the ISO 12640-2:2004 standard [28] and 8 CIELAB/SCID images from the ISO 12640-3 [29] (reproduced in Figure 6). Images were printed at a resolution of 150 pixels

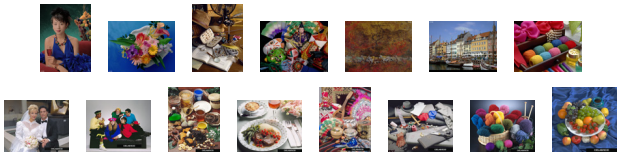

Figure 6. *sRGB images from ISO 12640-2 (top) and CIELAB/SCID images from ISO 12640-3 (bottom).*

per inch and a size of 1200 x 1500 pixels, 20.32 by 25.4 cm (i.e. 8 by 10 inches). The sRGB images were converted to CIELAB using the relative colorimetric intent of the sRGB profile. The CIELAB/SCID images are encoded in CIELAB colors. All the images were then gamut mapped in the CIELAB color space using the 5 different GMAs.

Output device and medium The destination gamut was the gamut of an Océ ColorWave 600 printer using Océ Red Label paper and the printer highest quality setting *Présentation mode*. It was measured by a spectrophotometer GretagMacbeth Spectroscan using GretagMacBeth MeasureTool 5.0.8. The resulting images were then converted from CIELAB to the device CMYK using the relative colorimetric intent of a custom printer CMYK ICC profile. They where printed on a Océ ColorWave 600 printer using Océ Red Label paper with the color management disabled.

Observers and Viewing Conditions The test panel was constituted by 8 female and 9 male observers with normal vision and various degree of expertise in judging image quality. The 5 printed gamut-mapped candidates were presented in a controlled viewing room with a lighting system at a color temperature of 5200 Kelvins, a illuminance level of 450 lux ± 75 and color rendering index of 96. Our aim was to carry a thorough evaluation by having two sets of images with different input color gamuts and reference reproduction devices. The observers viewed simultaneously the reference image and the printed images from a distance of approximately 60 cm.The experiment was then two-fold:

- For the sRGB image set, the observers were presented with a reference image on an EIZO ColorEdge CG221 display at a color temperature of 5200 Kelvins and luminance level of 120 cd/m^2. This set is rendered for sRGB display. Therefore a monitor capable of displaying the sRGB gamut is the most adapted reproduction device for this set of images.
- For the CIELAB/SCID image set, the observers were presented with a reference image printed on an Epson R800 printer using Epson Premium Glossy Photo Paper in the best printing quality mode. This set is rendered for the Perceptual Reference Medium Gamut (PRMG). The most appropriate way to reproduce these images is using a printing system able to reproduce the color gamut PRMG and with a good capability to reproduce details, such as the Epson R800 printer with Epson Premium Glossy Photo Paper.

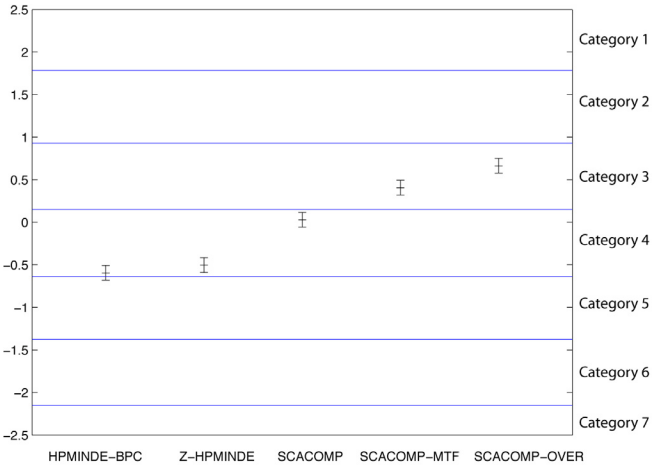

Figure 7. *Z-scores resulting of our experiment 2 (category scaling), average over 15 images and 17 observers.*

Global results Results cumulated over the 15 images and 17 observers in Figure 7 show that overall SCACOMP-OVER outperforms all other alternatives. The three versions of SCACOMP obtained the best scores, followed by Z-HPMINΔE and HPMINΔE at the same level. Each version of SCACOMP is perceived as significantly different from the others, from the top rated: SCACOMP-OVER, then SCACOMP-MTF and at last SCACOMP. SCACOMP-OVER, then SCACOMP-MTF are in category 3, SCACOMP, Z-HPMINΔE and HPMINΔE are in category 4. The ranking is identical when restricting the analysis to the set of 7 sRGB images. When considering only the 8 CIELAB/SCID images, the order changes as judgement for Z-HPMINΔE drops below HPMINΔE and to category 5.

Comments First it should be noted that this experiment was considered as hard by most observers, the difference between the alternative reproductions are not as striking as in the above statistical results. BPC was applied in the 5 alternative re-rendering and has lessen the impact of the subsequent GMAs by reducing the size of the input image gamut, leading to closer results. While these reduced differences are not welcomed by observers as the difficulty of the task increases, the quality of the worst of the five alternative reproductions (BPC+HPMINΔE) is sufficient to be implemented in real-world workflows and the quality gained by spatial gamut mapping algorithms provides an interesting added value. Statistically over the set of images, the observers tend to give the same judgment. With this experiment, we can conclude that Spatial GMAs produce results that are perceived as more accurate than pointwise GMAs. The difference lies mainly in saturated, dark areas or very light areas.

Conclusions

In this paper we have proposed an approach to compensate for the printer modulation transfer function within the spatial and color adaptive gamut mapping algorithms workflow. The category judgement experiment has delivered encouraging results. More studies remain necessary to fully apprehend the benefits and drawbacks of the MTF compensation and to find optimal parameters for over-compensation, including in the case of noisy images. The use of MTF compensation within a classic pointwise GMA workflow as well as in other imaging workflows should also be investigated.

References

[1] W. Jang and J. P. Allebach, "Characterization of printer MTF," in *Proceedings of SPIE , Image Quality and System Performance III, Luke C. Cui, Yoichi Miyake, Editors*, vol. 6059, pp. 1–12, 2006.

[2] J. Morovič and R. Luo, "The fundamentals of gamut mapping: A survey," *The Journal of Imaging Science and Technology, No.3*, vol. 45, pp. 283–290, 2001.

[3] J. J. McCann, "Color gamut mapping using spatial comparisons," in *Proc. SPIE, Color Imaging, VI*, vol. 4300, pp. 126–130, 2001.

[4] P.-L. Sun, *The Influence of Image Characteristics on Colour Gamut Mapping*. Derby, UK: University of Derby PhD Thesis, 2002.

[5] N. Bonnier, *Contributions to Spatial Gamut Mapping Algorithms.* Paris, France: Telecom ParisTech, PhD Thesis, 2008.

[6] R. Balasubramanian, R. de Queiroz, and R. Eschbach, "Gamut mapping to preserve spatial luminance variations," in *Eighth Color Imaging Conference: Color Science and Engineering Systems, Technologies, Applications*, vol. 1, (Scottsdale, Arizona), pp. 122–128, 2000.

[7] J. Morovič and Y. Wang, "A multi-resolution, full-colour spatial gamut mapping algorithm," in *11th IS&T/SID Color Imaging Conference*, pp. 282–287, 2003.

[8] I. Farup, C. Gatta, and A. Rizzi, "A multiscale framework for spatial gamut mapping," in *IEEE Transactions on Image Processing, No. 10, October 07*, vol. 16, pp. 2423–2435, 2007.

[9] S. Nakauchi, S. Hatanaka, and S. Usui, "Color gamut mapping based on a perceptual image difference measure," in *Color Research and Application*, vol. 24, pp. 280–290, 1999.

[10] P. Zolliker and K. Simon, "Adding local contrast to global gamut mapping algorithms," in *Third European Conference on Colour in Graphics, Imaging, and Vision (CGIV)*, vol. 1, (Leeds, UK), pp. 257–261, 2006.

[11] C. Liu, G. M. Johnson, and M. D. Fairchild, "Perception and modeling of halftone image quality using a high-resolution lcd," in *13th IS&T/SID Color Imaging Conference*, (Scottsdale, Arizona), pp. 165–170, 2005.

[12] N. Bonnier, F. Schmitt, H. Brettel, and S. Berche, "Evaluation of spatial gamut mapping algorithms," in *Proceedings of the14th IS&T/SID Color Imaging Conference*, vol. 1, (Scottsdale, Arizona), pp. 56–61, 2006.

[13] F. Dugay and I. Farup, "Perceptual evaluation of colour gamut mapping algorithms," in *Proceedings of Gjøvik Color Imaging Symposium*, (Gjøvik, Norway), 2007.

[14] N. Bonnier, F. Schmitt, M. Hull, and C. Leynadier, "Spatial and color adaptive gamut mapping: A mathematical framework and two new algorithms," in *Proceedings of the 15th IS&T/SID Color Imaging Conference*, vol. 1, (Albuquerque, NM), pp. 267–272, 2007.

[15] N. Bonnier, F. Schmitt, and C. Leynadier, "Improvements in spatial and color adaptive gamut mapping algorithms," in *Proceedings of IS&T/SPIE 4th European Conference on Colour in Graphics, Imaging and Vision*, (Terrassa-Barcelona, Spain), pp. 341–346, 2008.

[16] A. Lindner, N. Bonnier, F. Schmitt, and C. Leynadier, "Evaluation of characterization methods of printer MTF," in *Proceedings of the IS&T/SPIE Conference Electronic Imaging 2008*, vol. 6808, (San Jose, California), pp. 6808061–68080612, 2008.

[17] C. E. Shannon, "Communication in the presence of noise," *Proc. Institute of Radio Engineers*, vol. 37, pp. 10–21, 1949.

[18] ISO 12233, *ISO 12233:2000 Photography – Electronic still picture cameras – Resolution measurements*. ISO, 2000.

[19] ISO 16067-1, *ISO 16067-1:2003 Photography – Spatial resolution measurements of electronic scanners for photographic images – Part 1: Scanners for reflective media*. ISO, 2003.

[20] J. Arney, P. Anderson, P. Mehta, and K. Ayer, "The MTF of a printing systems," *IS&T's NIP16: International Conference on Digital Printing Technologies*, pp. 367–369, 2000.

[21] J. Hasegawa, T.-Y. Hwang, H.-C. Kim, D.-W. Kim, and M.-H. Choi, "Measurement-based objective metric for the printer resolution," in *Image Quality and System Performance IV. Edited by Cui, Luke C.; Miyake, Yoichi. Proceedings of the SPIE*, vol. 6494, p. 64940D, 2007.

[22] Y. Bang, S. H. Kim, and D. C. Choi, "Printer resolution measurement based on slanted edge method," in *Image Quality and System Performance V, Proc. of SPIE-IS&T Electronic Imaging*, 2008.

[23] A. Lindner, N. Bonnier, F. Schmitt, and C. Leynadier, "Measurement of printer MTFs," in *Submitted to IS&T/SPIE Conference Electronic Imaging 2009*, (San Jose, California), 2009.

[24] C. Tomasi and R. Manduchi, "Bilateral filtering for gray and color images," in *Proceedings of the Sixth International Conference on Computer Vision*, (Washington, DC, USA), p. 839, IEEE Computer Society, 1998.

[25] L. Borg and Adobe Systems, "Adobe systems implementation of black point compensation," in *http://www.color.org/AdobeBPC.pdf , downloaded 08/2007*, 2002.

[26] J. Morovič, *To Develop a Universal Gamut Mapping Algorithm.* Derby, UK: University of Derby, PhD Thesis, 1998.

[27] A. M. Bakke, "ICC3D.1.2.9," in *http://colorlab.hig.no/icc3d/ , downloaded 03/2007*, 2007.

[28] ISO 12640-2, *ISO 12640-2:2004 Graphic technology – Prepress digital data exchange – Part 2: XYZ/sRGB encoded standard colour image data (XYZ/SCID)*. ISO, 2004.

[29] ISO 12640-3, *ISO 12640-3:2007 Graphic technology – Prepress digital data exchange – Part 3: CIELAB standard colour image data (CIELAB/SCID)*. ISO, 2007.

Author Biography

Nicolas Bonnier is a color scientist with Océ Print Logic Technologies whom he represents in the International Color Consortium. He graduated from ENS Louis Lumière (Paris) in 2000, major in photography, and received his Master degree in Electronic Imaging from Université Pierre et Marie Curie (Paris) in 2001. He was a member of the Laboratory for Computational Vision with Pr Simoncelli at the New York University from 2002 to 2005. Then he completed a PhD program from 2005 to 2008 under the direction of Pr Schmitt, Télécom Paristech, sponsored by Océ.